Science of the Total Environment 859 (2023) 160080

Contents lists available at ScienceDirect

Science of the Total Environment

journal homepage: www.elsevier.com/locate/scitotenv

Co-exposure to UV radiation and crude oil increases acute embryotoxicity and sublethal malformations in the early life stages of Atlantic haddock (*Melanogrammus aeglefinus*)

Elin Sørhus [a,*], Carey E. Donald [a], Charlotte L. Nakken [b], Prescilla Perrichon [c], Caroline M.F. Durif [d], Steven Shema [e], Howard I. Browman [d], Anne Berit Skiftesvik [d], Kai K. Lie [a], Josef D. Rasinger [a], Mette H.B. Müller [f], Sonnich Meier [a]

[a] Institute of Marine Research, Marine Toxicology Group, Nordnesgaten 50, 5005 Bergen, Norway
[b] University of Bergen, Department of Chemistry, Allégaten 41, 5020 Bergen, Norway
[c] Institute of Marine Research, Reproduction and Developmental Biology, Austevoll Research Station, Sauganeset 16, 5392 Storebø, Norway
[d] Institute of Marine Research, Ecosystem Acoustics Group, Austevoll Research Station, Sauganeset 16, 5392 Storebø, Norway
[e] Grótti ehf, Melabraut 22, 220 Hafnarfirði, Iceland
[f] Norwegian University of Life Sciences, Section for Experimental Biomedicine, Universitetstunet 3, 1433 Ås, Norway

HIGHLIGHTS

- Co-exposure with oil and UV decreased acute LC50 by 60 %.
- Acute embryotoxicity was seen after onset of heart beat and only in the co-exposure.
- Very low oil levels (5–30 μg oil/L) in combination with UV led to sublethal defects.
- UV radiation degraded the outer membrane of Atlantic haddock eggs.

GRAPHICAL ABSTRACT

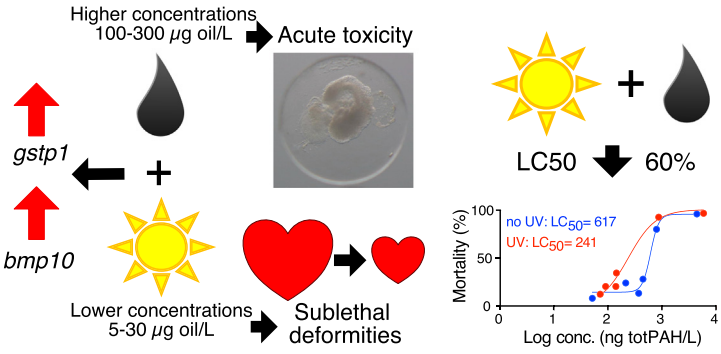

ARTICLE INFO

Editor: Henner Hollert

Keywords:
Crude oil
UV radiation
Early life stages of fish
Marine coldwater
PAH
BMD
LC50
Acute effects
Sublethal effects

ABSTRACT

Crude oil causes severe abnormalities in developing fish. Photomodification of constituents in crude oil increases its toxicity several fold. We report on the effect of crude oil, in combination with ultraviolet (UV) radiation, on Atlantic haddock (*Melanogrammus aeglefinus*) embryos. Accumulation of crude oil on the eggshell makes haddock embryos particularly susceptible to exposure. At high latitudes, they can be exposed to UV radiation many hours a day. Haddock embryos were exposed to crude oil (5–300 μg oil/L nominal loading concentrations) for three days in the presence and absence of UV radiation (290–400 nm). UV radiation partly degraded the eggs' outer membrane resulting in less accumulation of oil droplets in the treatment with highest oil concentration (300 μg oil/L). The co-exposure treatments resulted in acute toxicity, manifested by massive tissue necrosis and subsequent mortality, reducing LC50 at hatching stage by 60 % to 0.24 μg totPAH/L compared to 0.62 μg totPAH/L in crude oil only. In the treatment with nominal low oil concentrations (5–30 μg oil/L), only co-exposure to UV led to sublethal morphological heart defects. Including phototoxicity as a parameter in risk assessments of accidental oil spills is recommended.

* Corresponding author.
E-mail address: elins@hi.no (E. Sørhus).

http://dx.doi.org/10.1016/j.scitotenv.2022.160080
Received 29 August 2022; Received in revised form 28 October 2022; Accepted 5 November 2022
Available online 11 November 2022

1. Introduction

Crude oil is a complex mixture of thousands of different components. The toxicity of several of them, especially heterocycles and specific 3–5-ring polycyclic aromatic hydrocarbons, is increased by exposure to ultraviolet radiation (UV photoenhancement) (Barron, 2017; Roberts et al., 2017). Photoenhanced toxicity by chemical modification via photooxidation is referred to as photomodification, while photoexcitation within the animal is referred to as photosensitization (Barron, 2017). The early life stages of some fishes are translucent and, therefore, highly susceptible to photoexcitation of bioaccumulated photoexcitable residues. Photosensitization inside the organism creates free radicals including reactive oxygen species or other reactive products (Barron, 2017). An overload of free radicals triggers cellular dysfunction, lipid peroxidation, DNA mutagenesis and other oxidative stress pathways, leading to cell death and mortality (Barron, 2017; Takimoto and Kass, 2007). Exposure to crude oil in the presence of solar ultraviolet radiation (UV) exacerbates effects on embryogenesis (Barron, 2017; Sweet et al., 2017).

Accidental oil spills in the critical spawning habitats of fish are a recurring global problem (Allan et al., 2012; Ji et al., 2011; Peterson et al., 2003). Increased energy demand has resulted in increased oil extraction activity and proposals for increased activities in Arctic areas. This includes areas around the Lofoten Islands, in the Norwegian Arctic and in the Barents Sea (Misund and Olsen, 2013; Solsvik, 2022). These regions are especially vulnerable since they have a simple food web structure that is dependent on fewer key species compared to temperate areas making them more sensitive to anthropogenic impacts (Brown, 2014). Such regions are also important spawning and nursery grounds for several commercially important species of marine fish (Olsen et al., 2010). UV radiation is high in Arctic areas during spring and summer with 10–24 h of daylight in Lofoten islands (Date, 2021), with 600 kJ/m doses of 290–400 nm (Aranguren-Abadía et al., 2021). In addition, some of these regions are within the Arctic ozone hole area (Manney et al., 2011), further increasing UV radiation levels.

The main spawning area for Atlantic haddock (*Melanogrammus aeglefinus*) is near the Lofoten islands (Olsen et al., 2010). Haddock embryos have an extra outer membrane to which oil droplets adhere (Sørensen et al., 2017; Sørhus et al., 2021a; Sørhus et al., 2017; Sørhus et al., 2016), a characteristic that has also been observed in polar cod (*Boreogadus saida*) (Laurel et al., 2019), but not observed in other gadoids (Hansen et al., 2018; Morrison et al., 1999; Oppen-Berntsen et al., 1990). This trait results in an increased uptake into the haddock embryo that makes them approximately 10 times more sensitive to crude oil exposure than their close relative, the Atlantic cod (*Gadus morhua*) (Sørensen et al., 2017). Haddock embryos are pelagic (floating near the surface) (Solemdal et al., 1997) and the spawning season occurs in March/April when the number of hours of daylight exceeds ten. In that context, haddock are likely to be exposed to UV-radiation in large periods of their embryonic stage. The objective of this study was to evaluate the impact that co-exposure to crude oil and UV radiation has on haddock early development and survival.

2. Material and methods

2.1. Animal collection, management and exposure setup

A broodstock of Atlantic haddock was kept at the Austevoll Research Station of the Institute of Marine Research, Norway. Fertilized eggs were collected from the outflow of the broodstock tanks and kept in incubators at 8 ± 2 °C at a salinity of 34 ‰ before transfer to exposure tanks (~6000 eggs per tank, 72,000 eggs in total). The intake of sea water to the Austevoll Research Station is at 160 m depth and has a capacity of 10,000 L/min.

Exposure was performed following the methods described in Aranguren-Abadía et al. (2021). However medium and high concentrations were reduced by 50 % due to the high sensitivity of haddock embryos to crude oil. In short, seawater flow in 50 L green plastic tanks (one tank per treatment) was 32 L/h and the temperature of the seawater was maintained at 8 ± 2 °C at a salinity of 34 ‰. The crude oil used in the study was obtained from SINTEF Materials and Chemistry (Trondheim, Norway) and originates from the Troll field in the North Sea. Before exposure, the crude oil was heated for about 2 h at 200 °C to remove light and volatile substances present in crude oil, similar to what would evaporate from the sea surface after 2–7 days at around 10 °C air temperature. Doing this resulted in a more environmentally relevant exposure (Nordtug et al., 2011). Preparation of oil in water dispersion and exposure regime was identical to previous experiments (Sørhus et al., 2016). The exposure system and the generation and delivery of oil droplets is described in detail by Nordtug et al. (2011). In brief, the crude oil was pumped into the dispersion system using a HPLC pump (LC-20 AD, Shimadzu) with a flow of 0.01 mL/min combined into a 180 mL/min flow of seawater. This system generates oil dispersion with oil droplets in the low μm size range at a nominal oil load of 46 mg/mL (stock solution). A parallel pipeline system consisting of one line of flowing seawater and one line containing the stock solution regulated the amount of oil dispersion that entered each tank. The two pipelines were connected by a 3-way magnetic valve allowing collection of water from both lines. Different dilutions were produced by controlling the relative sampling time from the oil stock solution and clean water, respectively, using a computer-controlled relay (MiniBee card and BeeStep software).

Two experiments were conducted simultaneously: i) one with crude oil exposure without UV light (oil-noUV) and ii) another one with crude oil exposure combined with UV light exposure (oil-UV). The concentrations of oil applied in this study were intended to recreate those found in a real-life exposure scenario. For example, in the Deepwater Horizon oil spill, PAH concentrations were around 100 μg PAH/L close to the wellhead, while levels in surrounding areas (up to 20 km from the wellhead) had concentrations of 0.1–10 μg PAH/L (Boehm et al., 2016). Considering that PAHs make up about 1.6 % of the crude oil (Hansen et al., 2019; Meador and Nahrgang, 2019), 0.1–10 μg PAH/L corresponds to approximately 6–600 μg oil/L. Nominal crude oil concentrations were therefore set to: 5 μg oil/L (Low concentration 1; L1), 10 μg oil/L (Low concentration 2; L2), 30 μg oil/L (Low concentration 3; L3), 100 μg oil/L (Medium concentration; M), 100 μg oil/L filtered (Medium concentration water soluble fraction; M-oil-WSF) and 300 μg oil/L (High concentration; H). In addition, we had two tanks with no oil (0 μg oil/L)—one without UV (C-noUV) and one with UV (C-UV) (Fig. 1). Although we aimed for the same nominal concentrations in the crude oil vs UV co-exposed treatments, in the low concentrations (L1, L2, and L3), the time of valve opening was very short (few seconds), creating variability in the amount of oil entering the tank. Therefore, the concentration of oil in the water of those treatments was sampled daily throughout the exposure period (Dataset S1). Exposure started at 3 days post fertilization (dpf) from early gastrulation and lasted for 72 h (h) until 6 dpf, when the formation of the cardiac cone prior to the tubular heart begins (Fridgeirsson, 1978; Hall et al., 2004). After exposure, all surviving embryos were transferred to new 50 L tanks (one tank per treatment) with clean seawater using meshed cylinders. The UV light exposure (12 h light/dark) continued until the termination of experiment at 3 days post hatch (dph). All incubation tanks were illuminated using two 40 W fluorescent lamps. The UV-exposed tanks had two additional 40 W Q-Panel fluorescent bulbs (UVA-340 Q-Lab, Westlake, Ohio, USA; the UV irradiance is centered at 340 nm) suspended beneath the standard white light fluorescents. To ensure a stable spectral output in the UV-exposure, the Q-Panel lamps were aged for 100 h before the experiment began. The target values for the UV radiation were determined based on data from the ALOMAR observatory at Andenes (Andøya, Lofoten, 69°18′N) and the U.S. National Science Foundation observatory at Barrow, Alaska (71°19′N), which are located at similar latitudes (http://uv.biospherical.com/login/data_overview.asp). The targeted daily doses of UV (290–400) were 600 kJ/m. The bulbs delivered this amount of UV radiation over a 12-hour period (12 h light/12 h dark) at an average flux of 14 ± W/m. Details regarding measuring the UV-exposure and illumination are presented in Aranguren-Abadía et al. (2021).

Mortality in the various treatments was calculated shortly after 100 % hatch. Non-linear regressions for mortality vs log concentration (ng totPAH/L) and mortality vs tissue content (bodyburden) (μg totPAH/kg) were calculated using PrismGraph (Prism9, version 9.3.1). In addition, benchmark doses (BMD) for 10 % and 50 % mortality were modelled and calculated using the PROASTweb module, Version 70.1. The model fit was evaluated by Akaike information criterion (AIC) and Extract Log-likelihood (Loglik) in the software.

2.2. Analytical chemistry

One liter of water was collected from each exposure tank at 24 h post exposure start (hpes), 48 hpes and 72 hpes. Water was preserved with HCl (pH < 2) and stored at 4 °C in the dark until further handling (no longer than 6 weeks). Procedures were executed as described in Sørensen et al. (2017). In short, the water samples were extracted twice by partitioning to dichloromethane. The extracts were then combined and concentrated for analysis by GC–MS/MS. Prior to extraction deuterated internal standards (naphthalene-d8, biphenyl-d8, acenaphthylene-d8, anthracene-d10, pyrene-d10, perylene-d12 and indeno[1,2,3-c,d]perylene-d12) were added to account for analyte loss during extraction. Measured 2–5 ring PAH compounds included 61 individual PAHs and 24 clusters representing sums of alkylated PAHs.

Three pooled samples per treatment of 50–100 embryos were collected at 24, 48, 72 and 96 hpes to detect changes in tissue uptake of PAHs. Images of each sample pool were acquired to establish the exact number of embryos that were used for normalization after analysis. Embryos were rinsed several times in clean sea water before flash freezing in liquid nitrogen. Extraction of tissue samples was performed by solid-liquid extraction followed by solid phase clean up before analysis on an Agilent 7890 gas chromatograph coupled to an Agilent 7010c triple quadrupole mass detector.

The weathered Troll oil in the present study was diluted, measured and found to contain 1.6 % PAHs, by weight (Hansen et al., 2019). The PAHs and alkylated homologues remain one of the few groups of oil compounds for which reliable and sensitive analytical methods for detection in relevant environmental matrices (e.g. water, sediments, biota) exist (Magi and Di Carro, 2018; Sørensen et al., 2016; Wu et al., 2019). The content of PAHs in crude oil correlates with toxicity in developing fish (Adams et al., 2014; Carls and Meador, 2009; Sørhus et al., 2021a). Therefore, PAH concentration is used as a proxy for crude oil exposure in this study.

2.3. Morphological and functional measurements

Un-anaesthetized larvae were immobilized in 3 % methylcellulose/97 % seawater and positioned on a thermally regulated microscope stage (Brook Industries, Lake Villa, IL) at 8 °C. Digital images were taken using a Moticam 1080 camera (Motic®, Richmond, BC, Canada) mounted on Olympus SZX10 stereomicroscope. Images were collected at 24, 48, 72, 96 and 120 hpes for medium concentrations and control, and at the end of exposure (72 hpes) and at 3 dph for all treatments and concentrations (Fig. 1). In addition, a few videos representing the general observations of abnormalities seen during image capturing in the various treatments were collected at 120 hpes. Cardiac morphology was obtained from 20-s videos captured at 3 dph. Due to indications of sampling related induced stress in all treatments, cardiofunctional data (contractility and heart rate) from the video analysis was not conducted because it would not have been an accurate reflection of treatment-induced effects.

Morphometry data (myotome length (μm), eye to front (μm), jaw length (μm) and eye, body and yolk area (μm^2)) from the 3 dph larval images were acquired by automated machine learning techniques (Kvæstad et al., 2022). All images were quality checked manually after completion of automated analysis. Ventricular areas (mm^2) were acquired from the videos and processed using imageJ software version 1.50 h (Schneider et al., 2012). Spinal,

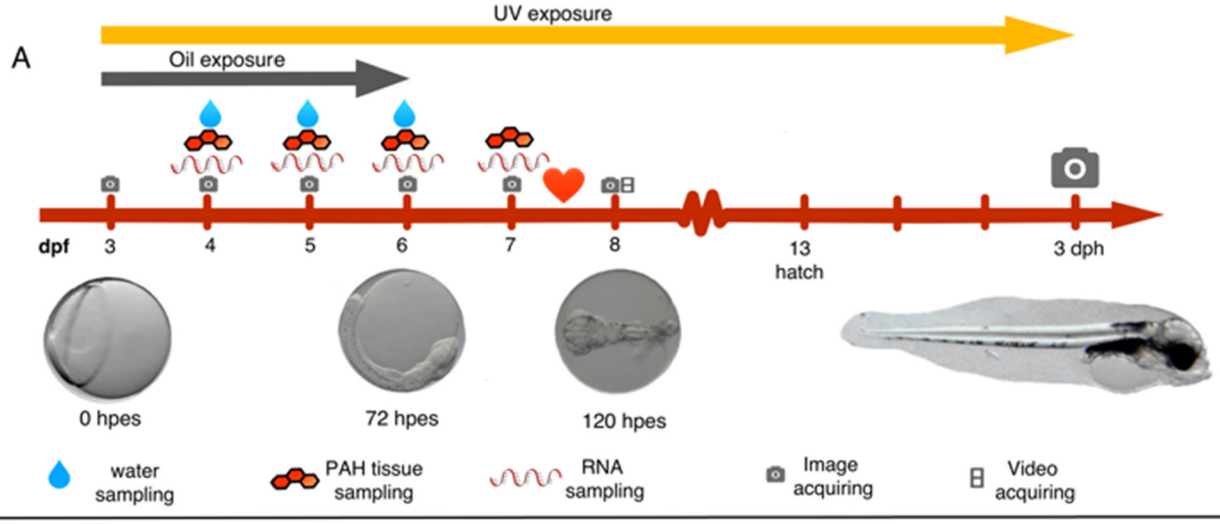

B

	Without oil	With oil					With oil no oil droplets
	Control	Low conc. 1 (5 μg oil/L)	Low conc. 2 (10 μg oil/L)	Low conc. 3 (30 μg oil/L)	Medium conc. (100 μg oil/L)	High conc. (300 μg oil/L)	Medium conc. (100 μg oil/L)
Without UV	C-noUV	L1-oil-noUV	L2-oil-noUV	L3-oil-noUV	M-oil-noUV	H-oil-noUV	M-oil-WSF
With UV	C-UV	L1-oil-UV	L2-oil-UV	L3-oil-UV	M-oil-UV	H-oil-UV	

Fig. 1. Experimental design. A) The oil exposure Atlantic haddock started at 3 dpf (0 hpes) and ended at 6 dpf (72 hpes). UV exposure started at 3 dpf and ended at the termination of the experiment at 3 dph. Large camera symbol: Imaging of 30 individuals per treatment. Small camera and video symbols: representative images and videos from the treatments. Hpes; hours post exposure start. B) Exposure (UV and oil) conditions applied in the experiment; there was one 50 L tank per treatment.

craniofacial and eye abnormalities were categorized (see detailed phenotypes in Fig. S1). Four spinal phenotypes were classified (Fig. S1A–D): Normal, hunched, arched and curved spines. Craniofacial phenotypes were grouped into five categories based on severity (Fig. S1E–I): Bulldog with reduced upper jaw, Jaw Breaker with posteriorly displaced jaws, Darth Vader with reduced upper and hanging lower jaws and Hunchback with severe reduction of all jaw structures. Three eye shape phenotypes were described (Fig. S1J-M): normal, bend shape (one indent) irregular shape and protruding lens. Analyses of control and treatment groups were performed blind.

2.4. Electron microscopy

Eggs were collected for scanning electron microscopy at 24 and 72 hpes from all concentrations and controls. Eggs were fixed in a Karnovsky's fixative (mixture of glutaraldehyde and formaldehyde), washed in PIPES buffer, dehydrated in a graded series of ethanol (15 min in each of the following concentrations: 30 %, 50 %, 70 %, 90 %, 96 %, and 100 %, repeating 100 % four times), before critical point drying (CPD 030, Bal-Tec, Germany) and Au-Pd coating using a Polaron Sputter Coater (SC7640, UK). Eggshell membranes were examined and photographed with a Zeiss EVO 50 EP scanning electron microscope.

2.5. Analysis of gene expression changes

Embryos were collected for RNA extraction at 24, 48, 72, 96 hpes from medium concentrations and control, and at 72 hpes (i.e., at the end of exposure) for all treatments (Fig. 1). Between 10 and 15 embryos were frozen in liquid nitrogen after imaging. See Text S1 in Supporting Information for details regarding extraction.

Specific Atlantic haddock primers and probes for RT-qPCR analysis were designed with Primer Express software (Applied Biosystems, Carlsbad, California, USA) (*cyp1a*, *gstp1* and the technical reference Elongation factor 1 alpha (*ef1a*)) or Integrated DNA Technology probe and primer design software (IDT Inc., Iowa, USA) (*cyp1b*, *cyp1c*, *bmp10* and technical reference Retinoic acid receptor RXR beta A (*rxrba*)), according to the manufacturer's guidelines. Sequences and additional details regarding RT-qPCR are given in Table S1 and Text S1. Changes in gene expression were calculated relative to the control values in the first sampling point using the ΔΔΔCt method (by generation of reference residuals from *ef1a* and *rxrba*) as described in detail in Edmunds et al., 2014.

2.6. Statistics

Statistical differences between treatments in PAH water concentration, PAH tissue uptake, changes in gene expression and morphology were tested using one-way ANOVA with Dunnett's and Tukey-Kramers multiple comparisons using R (The R Foundation for Statistical Computing Platform (packages: carData, multcomp)) after testing for normality using Shapiro-Wilk test in R. PAH concentration in water and tissue and changes in gene expression data were log-transformed before statistical testing due to large differences in concentrations and thus large standard deviation. In spinal, craniofacial and eye phenotypes, statistical differences between treatments and control (without UV) (C-noUV) were evaluated using chi-square test.

2.7. Ethics statement

All sampled embryos and yolk sac larvae were euthanized in liquid nitrogen immediately after imaging. The Austevoll Aquaculture Research station has the following permission for collecting and maintaining adult Atlantic haddock: H-AV 77, H-AV 78 and H-AV 79. The permits are issued by the Norwegian Directorate of Fisheries. No approval is necessary to perform studies with fish embryos and yolk sac larvae (prior to exogenous feeding). Nevertheless, the Austevoll Aquaculture Research station has a permit to operate as a Research Animal facility using all developmental stages of fish, with code 93 from the national Institutional Animal Care and Use Committee; National Animal Rights Association.

3. Results and discussion

3.1. Concentration of PAH in water and tissue and cyp1a expression changes

The exposure system delivered oil exposures consisting of oil microdroplets and the water soluble fraction to the oil-noUV and oil-UV treatments. There was some variation in the oil delivered, as shown by measured PAH concentrations (Fig. 2A). Total PAH concentrations in water were slightly lower in the M- and H-oil-noUV treatments, with an average of 0.8 and 4.5 μg PAH/L, respectively, compared to 0.9 (M-oil-UV) and 5.8 (H-oil-UV) μg PAH/L (Fig. 2A, Dataset S1). The concentration of PAHs in water in M-oil-WSF was 30 % lower than in M-oil-noUV (Fig. 2A), suggesting that about 30 % of the PAH load in the unfiltered treatments was present in oil droplets.

Trends with PAH uptake into tissues varied considerably depending on the presence of UV. In the high exposures, uptake was higher without UV (Fig. 2B, D, Dataset S2, Fig. S2). In the medium exposures, however, this difference was not as prominent (Fig. 2B, D, Dataset S2). These findings are in accordance with the observations that UV appears to degrade the “sticky” outer membrane of the egg (see Section 3.3). More oil droplets adhered to the eggshells, especially in the H-oil-noUV treatment, resulting in higher apparent PAH tissue concentrations. Accordingly, the greatest tissue concentrations were measured in H-oil-noUV. Compared to high, the medium treatments had less oil adhered to the eggshell as droplets, and therefore the PAH tissue uptake more closely followed water concentrations and was similar between UV and noUV (Fig. 2D). See further discussion below. In an analogous study in cod, the uptake in the noUV-treatment was also greater than the UV-treatment, suggesting that UV itself also affects the tissue uptake, through photomodification of the adsorbed PAHs (Aranguren-Abadía et al., 2021). However, the total tissue uptake in cod was 10 times lower than in the present study with haddock, the species previously reported of having the sticky eggshell (Sørensen et al., 2017; Sørhus et al., 2015). In haddock, we cannot discern whether increased photomodification or reduced oil droplet adhesion plays a larger role in reduced tissue concentrations of PAHs in the UV treatment.

Among the lower concentrations, uptake of PAHs into tissue was a more sensitive measure of exposure than concentrations in water. For example, the PAH level in the water of the L1-oil-UV treatment was not different than control (Fig. 2A), but the uptake of PAHs in the tissue was significantly higher than controls (Dataset S2, Fig. 2B).

Induction of cytochrome P450 1a (Cyp1a) is a sensitive biomarker for crude oil toxicity (Goksøyr, 1995; Harding et al., 2020). Oil droplets adhering to the sticky eggshell of haddock have shown to increase the uptake of PAHs followed by increased expression of *cyp1a* (Sørhus et al., 2021a). The oil-noUV treatments showed a higher *cyp1a* expression relative to tissue concentration of PAHs compared to the oil-UV treatments (Fig. 2E) reflecting more accumulation of oil droplets on the H-oil-noUV treatment. While tissue-PAH and therefore also calculation of bioconcentration factor may reflect oil residues both on the outside of the chorion that were not removed with washing and inside the embryo, detection of changes in *cyp1a* expression is an accurate indicator of the exposure the embryo was subjected to. This is displayed by the plateau in *cyp1a* expression observed in both noUV and UV *cyp1a*-tissue PAH correlation (Fig. 2E). Further, the degradation of the sticky eggshell and elimination of oil droplets on the chorion in the H-oil-UV treatment (see Section 3.3) resulted in both lower *cyp1a* expression changes and tissue content of PAH (Figs. 2, 3A and S2). This observation supports that oil components on the eggshell are also transferred to the embryo.

3.2. Gene expression changes indicates increased oxidative stress and calcium flux alterations in oil-UV treatments

Analysis of gene expression changes was performed with the M-concentrations, C-noUV and C-UV at all time points (Fig. 3), while the remaining treatments were evaluated only at 72 hpes (Fig. S3). No treatment-induced changes in expression of *cyp1b* were observed at any

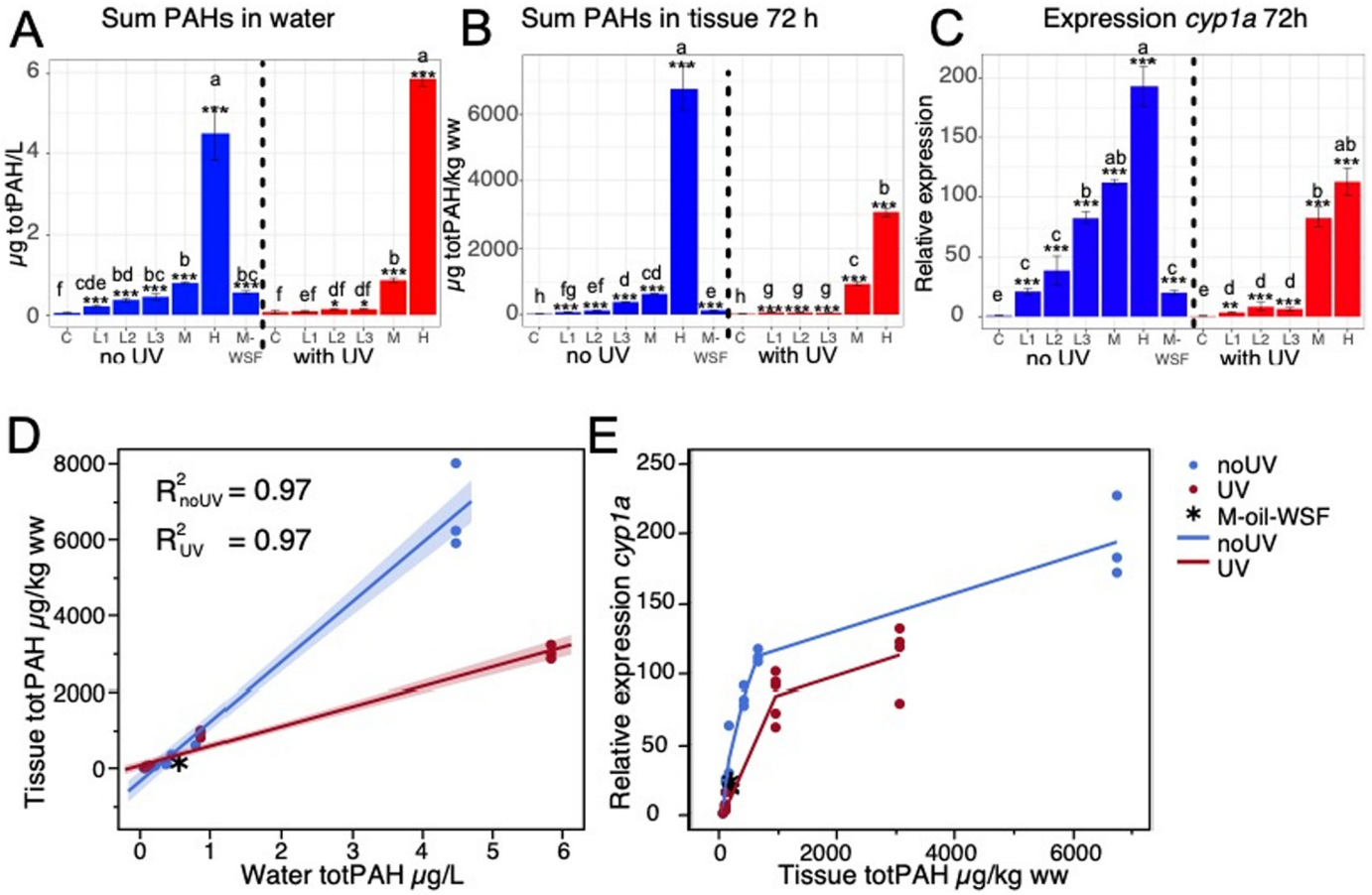

Fig. 2. Tissue uptake of PAH, water concentrations of PAH and cyp1a expression changes. A) Average total PAH in the water during the exposure (average of 24, 48 and 72 h), B) total PAHs in tissue and C) expression of cyp1a in all treatments at 72 h after the start of exposure (hpes). D) Tissue uptake of PAH (at 72 hpes) relative to PAH water concentrations (average of 24, 48 and 72 hpes), fitted to linear regressions: $R^2_{noUV} = 0.97$ and $R^2_{UV} = 0.97$. B) Expression changes of cyp1a relative to average tissue uptake of PAH (at 72 hpes), with lines drawn connecting the averages. Statistically significant differences between treatments and control (C-noUV) were tested for using one-way ANOVA and Dunnett's multiple comparison test at each time point. Statistical differences are indicated by ***$p < 0.001$. Differences between all treatments were tested using Tukey-Kramer's multiple comparisons. Differences are indicated by different letters ($p < 0.05$).

time-point (Fig. 3B, Fig. S3A). Changes in expression of *cyp1c* followed the same trend as *cyp1a* and increased in all treatments except L1-oil-UV and L2-oil-UV (Figs. 2C, 3A, C and S3B). This is consistent with previous experiments in which *cyp1a* and *cyp1c* were induced by oil exposure, while *cyp1b* was mainly induced by developmental events (Sørhus et al., 2021a). Gluthatione-S-transferase P1 (*gstp1*) is an important enzyme involved in the conjugation step (phase II) in xenobotic metabolism. By conjugating reactive activated metabolites, it contributes to reduce oxidative stress (Li et al., 2013). Thus, we expected oxidative stress to induce increased expression of *gstp1* in our treatments. Higher levels of *gstp1* were only observed in the high and medium treatments (Fig. 3D, Fig. S3C), suggesting that co-exposure led to more oxidative stress in the animals. This is consistent with the transcriptome analysis at 72 hpes in cod, which showed activation of oxidative stress pathways in the UV co-exposure treatments (Aranguren-Abadía et al., 2021).

Calcium is a ubiquitous second messenger that is involved in multiple cellular functions including contraction, metabolism and gene expression (Bagur and Hajnóczky, 2017). Previous studies linked crude oil induction of the calcium regulated protein bone morphogenetic protein 10 (Bmp10) in early embryonic development (6 dpf) to severe cardiac malformations in early larval stages (3 dph) (Sørhus et al., 2017). Oxidative stress increases the influx of Ca^{2+} into the cytoplasm from both the extracellular environment and from internal stores (endoplasmic/sarcoplasmic reticulum) (Görlach et al., 2015; Guo et al., 2013). We observed increased expression of *bmp10* in the M-oil-UV treatment at 72 hpes and 96 hpes in the timeline series (Fig. 3E). However, at 72 hpes, overexpression was only detected in the H-oil-no UV ($p < 0.001$), and M-and H-oil-UV ($p < 0.1$) treatments (Fig. S3D). These observations suggest that either relatively high oil concentrations or UV co-exposure is necessary to impact calcium induced regulation of *bmp10* expression.

3.3. UV increases the toxicity of crude oil to haddock embryos

In haddock, the adhesive extra outer egg membrane accumulates oil droplets (Sørensen et al., 2017; Sørhus et al., 2021a; Sørhus et al., 2015; Sørhus et al., 2016). Exposure to UV degraded the adhesive hydrophobic outer membrane of haddock embryos (Fig. 4A). Consequently, fewer oil droplets were evident on the chorion in the H-oil-UV treatment after 72 h of exposure (Fig. 4B and C), corroborated by reduced PAH tissue uptake (Figs. 2B, S2) and expression changes of *cyp1a* and *cyp1c* (Figs. 2C, 3A and C). In the M-oil-UV treatment, we observed that the oil covered area was similar to M-oil-noUV (Fig. 4D). Photomodification and photodegradation of oil components occurs when they are exposed to solar UV radiation (Bertilsson and Widenfalk, 2002; Roberts et al., 2017). Photomodification of oil suspended in the water might have been minimized in this study due to the high flowthrough (50 L tank with flow of 32 L/h). However, in haddock, photolytic conversion of oil components can occur in the oil droplets on the eggshell (photomodification) or inside the embryo (photosensitization). This may result in a *cyp1a*-independent photoinduced metabolism of oil components. Accordingly, we observed less expression changes of *cyp1a* in the M-oil-UV treatment (Figs. 2C, 3A), even though the content of PAH in the tissue was higher (Figs. 2B and S2).

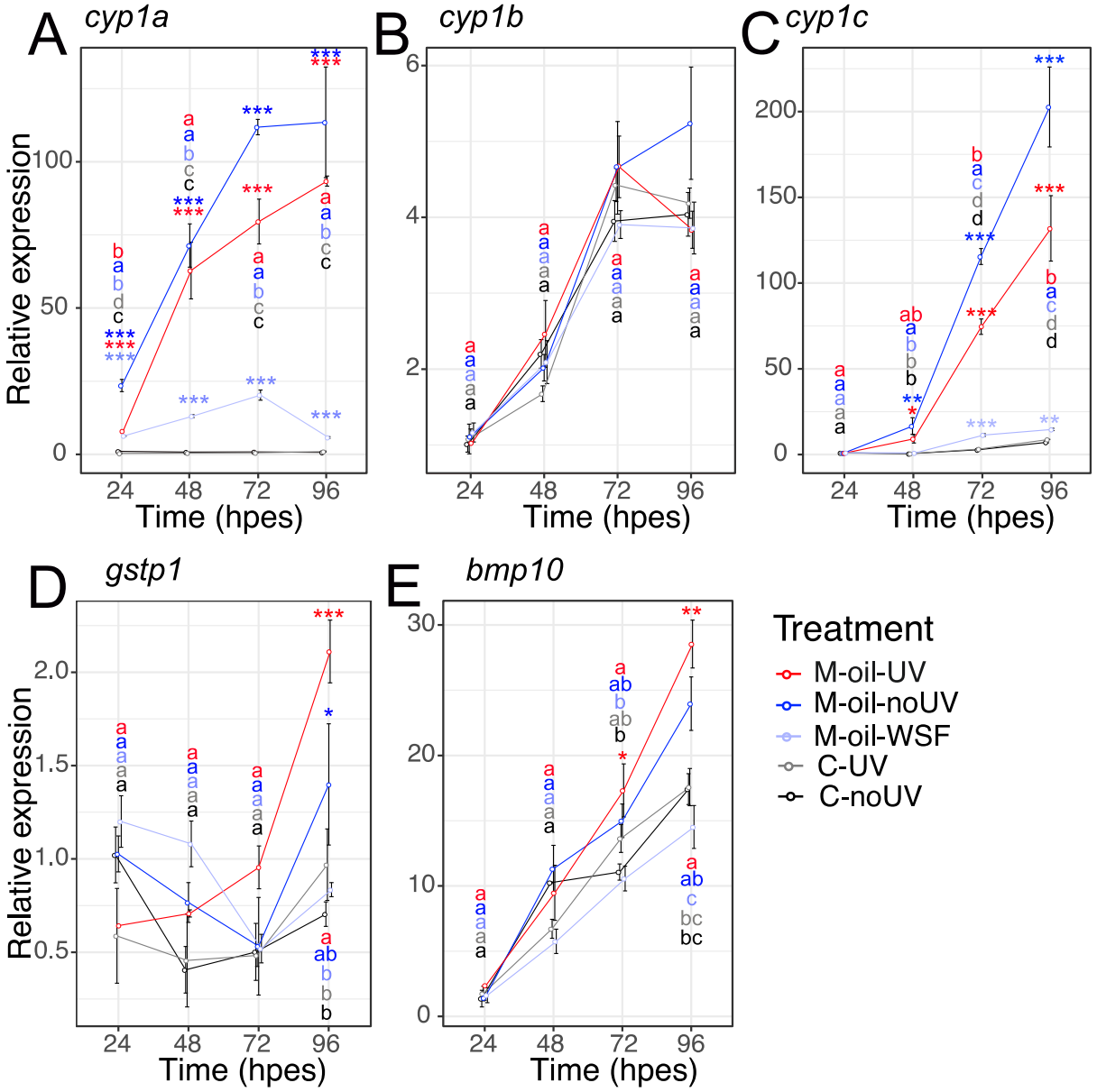

Fig. 3. Gene expression changes over time in 100 μg oil/L treatments and control. Expression changes of A) cyp1a, B) cyp1b, C) cyp1c, D) gstp1, E) bmp10. Statistical differences from C-noUV at each time-point were tested with one-way ANOVA and Dunnett's multiple comparison test and differences are indicated by $*p < 0.05$, $**p < 0.01$ and $***p < 0.001$. Differences between all treatments were tested with Tukey-Kramer's multiple comparison and differences are indicated by different letters ($p < 0.05$). Hpes; hours post exposure start.

Despite less accumulation of oil droplets on the chorion, embryotoxicity was increased by UV exposure. Acute toxicity, i.e. large scale accumulation of edema, necrosis and dying embryos (Fig. 4E and Fig. S4) were only observed in the medium and high oil-UV treatments (90 % and 60 % in the H-oil-UV and M-oil-UV, respectively, at 120 hpes). Photoenhanced acute toxicity has been observed in several other species (Aranguren-Abadía et al., 2021; Barron, 2017; Barron et al., 2003; Incardona et al., 2012a; Incardona et al., 2012b). Rapid loss of cellular integrity and disintegration were observed in Pacific herring (*Clupea pallasii*) embryos exposed to bunker and crude oil in combination with UV radiation (Barron et al., 2003; Incardona et al., 2012a; Incardona et al., 2012b). Very short periods (2.5 h/d for 2 days) of sunlight together with crude oil was sufficient to cause an order of magnitude higher toxicity than crude oil alone (Barron et al., 2003). The very rapid cell death and total degradation of the organ structures that were observed in the oil-UV embryos (Fig. S4) suggest that this is mediated through a massive necrosis mechanism (Chilakamarthi and Giribabu, 2017; Edinger and Thompson, 2004). However, programmed cell death, like apoptosis (Leads et al., 2022) and ferroptosis (Aranguren-Abadía et al., 2021) are also mechanisms that have been reported after co-exposure of oil and UV radiation in fish embryos/larvae.

At the end of exposure (72 hpes), all UV treated animals (including C-UV) had vesicles at the tail end of the embryo (Fig. 4D). This was not observed in the noUV treatments. Small extracellular vesicles are produced by human melanoma cells in response to oxidative stress (Harmati et al., 2019). Oxidative stress can negatively affect organisms in several ways (Takimoto and Kass, 2007). For example, increased cytoplasmic calcium levels induced by oxidative stress will increase the Ca^{2+} influx into mitochondria and nuclei. Disruption of mitochondrial calcium homeostasis accelerates and disrupts normal metabolism leading to cell death (Ermak and Davies, 2002; Görlach et al., 2015). In addition, peroxidation of membrane lipids results in cellular dysfunction and reactive oxygen species cause mitochondrial dysfunction by damaging important enzymes in the respiratory chain (Ott et al., 2007; Takimoto and Kass, 2007). Thus, we suggest that the vesicle formation, followed by acute toxicity and death, may

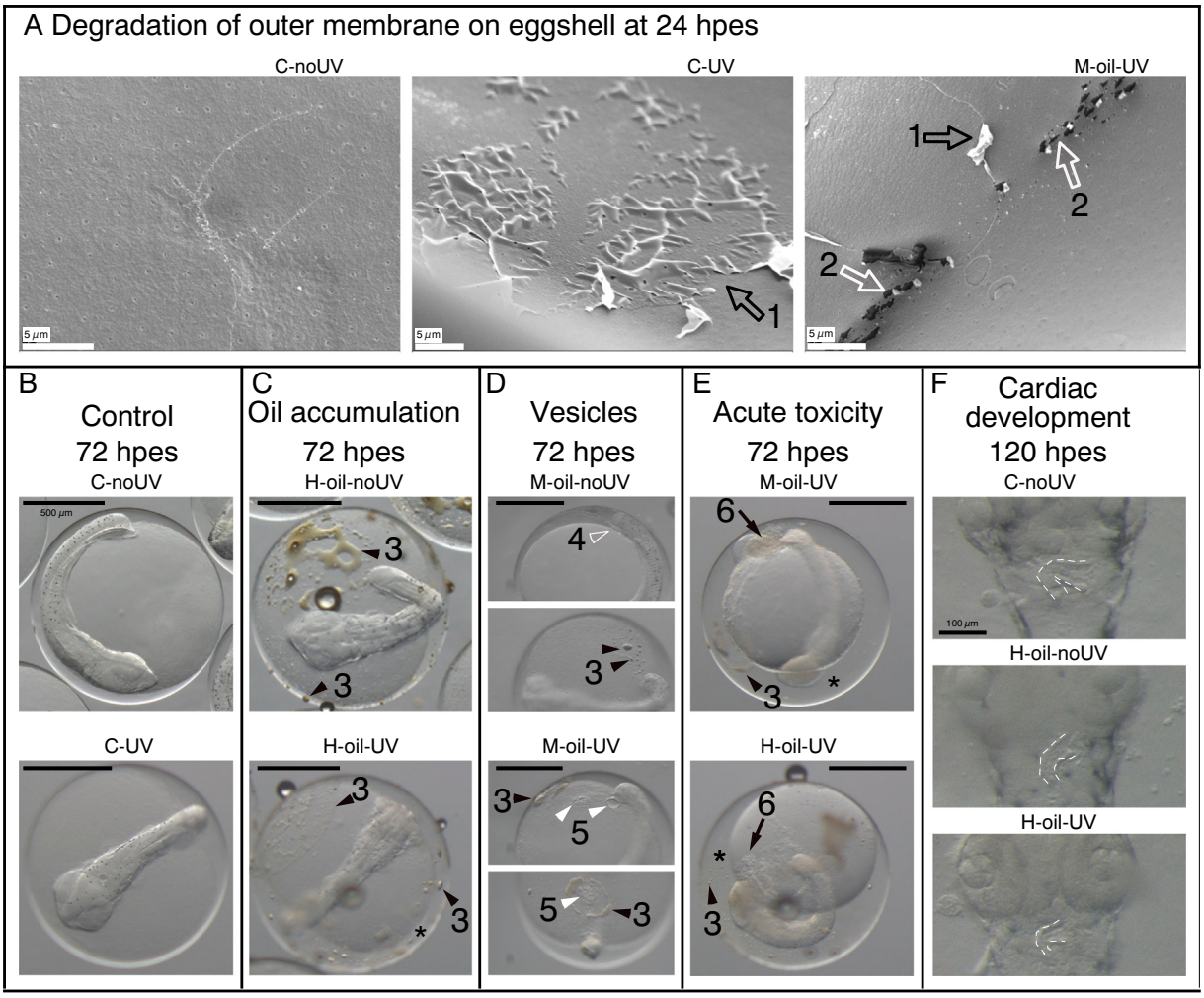

Fig. 4. Atlantic haddock embryos exposed to oil with and without UV. A) Electron microscope images of the eggshell of haddock (24 hpes) showing that exposure to UV degraded the adhesive hydrophobic outer membrane. Scale bar: 5 μm. B) Control haddock embryos (6 dpf) at the exposure stop (72 hpes). C) Accumulation of oil droplets on the chorion of the highest concentration (300 μg oil/L) in 72 hpes embryos with and without UV. D) Vesicle formation in M-oil-UV but not in M-oil-noUV at 72 hpes. E) Acute toxicity and dying embryos (72 hpes) in the co-exposure. Scale bar B-E: 500 μm. F) Heart shape in representative embryos of C-noUV, H-oil-noUV and H-oil-UV (120 hpes). Scale bar: 100 μm. Corresponding videos: Supplementary video 1–6. 1: degradation of outer membrane. 2: most likely deep ruptures in the membrane. 3: accumulation of oil droplets. 4: no vesicle formation. 5: formation of vesicles. 6: necrosis of embryo. Asterisk: edema. Dotted line: outline of heart shape.

also be the result of photoinduced oxidative stress in the UV co-exposed animals.

Crude oil impacts cardiac development and function (Incardona et al., 2021; Perrichon et al., 2018; Pasparakis et al., 2019; Sørhus et al., 2021a; Sørhus et al., 2016; Sørhus et al., 2021b). Two days after exposure ended, at 120 hpes, the hearts in the high concentration treatments were smaller and were less looped. Though the looping abnormalities were more apparent in the H-oil-noUV, the size of the heart was smaller in the H-oil-UV treatment (Fig. 4F). Similarly, initiation of cardiac function had occurred in all treatments and controls at 120 hpes except in the co-exposed high treatment H-oil-UV (Supp. concatenated video), suggesting delayed cardiac development. Oxidative stress affects multiple molecular signaling pathways important for cardiac development and function. Cardiac hypertrophy and remodeling have been linked to molecular impacts on calcium channels, α and β adrenergic receptors, sarcomeric and excitation-contraction coupling proteins, nuclear transcription factors and many more (Takimoto and Kass, 2007). Oxidative stress pathways were activated in co-exposed cod embryos (Aranguren-Abadía et al., 2021). When exposure ended (6 dpf), the pre-stage of the heart tube (cardiac cone) in the UV co-exposed groups was not observed (Aranguren-Abadía et al., 2021), indicating delayed or disrupted cardiac development. In this study, both *gstp1* and *bmp10* were up-regulated in the oil-UV treatments confirming increased xenobiotic activity and impact on calcium regulated transcription. Thus, photo-induced oxidative stress appears to exacerbate the delay in cardiac development in oil-UV animals.

3.4. Oil and UV induced morphological abnormalities and mortality

Severe crude oil induced morphological defects were observed in 3 dph larvae in all exposure treatments (Fig. 5). The abnormalities seen in haddock were much more severe than those observed in Atlantic cod using the same exposure setup (Aranguren-Abadía et al., 2021), even though the two highest concentrations used in the present study were 50 % lower. More morphological abnormalities were observed with increasing crude oil concentration, regardless of UV exposure. The M-oil-WSF (without oil droplets) was an exception: no abnormalities were seen. At hatching, the mortality was over 80 % in the medium and high treatments (with oil droplets) (Fig. 5L) and no animals survived to 3 dph in the co-exposed medium and high treatments. UV-radiation interacts with components in the oil and increases toxicity from 2 to 1000-fold (Aranguren-Abadía et al., 2021; Barron, 2017; Barron et al., 2005). Accordingly, the acute toxicity was much higher in the oil-UV treatments during the entire embryonic

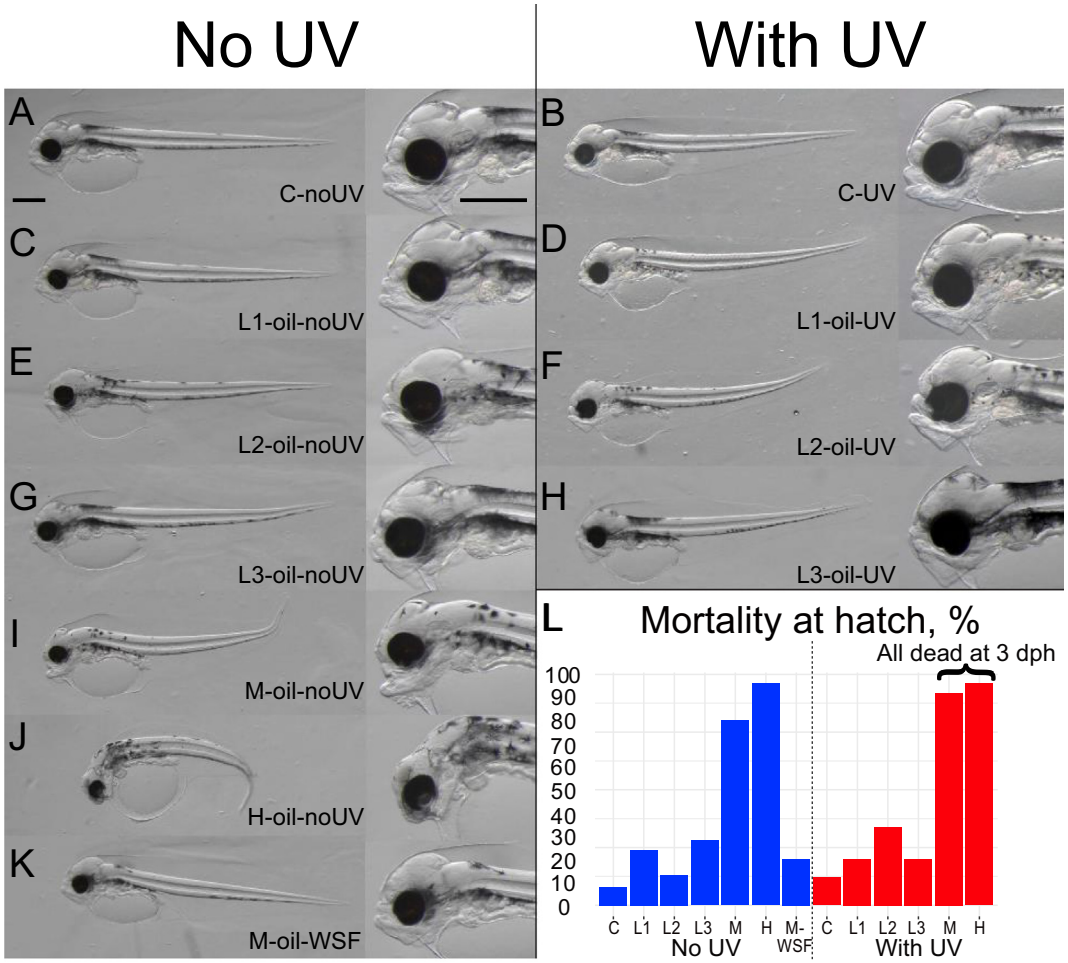

Fig. 5. Phenotypes in 3 days post hatch (dph) Atlantic haddock larvae exposed during the early embryonic stage. A–J) Increasing malformations were seen with increasing oil concentrations and UV. K) Exposure to M-oil-WSF resulted in very few abnormalities. L) Mortality at hatch (%), no larvae from M-oil UV and H-oil-UV survived to 3 dph.

stage (Fig. S4). In Pacific herring, acute embryonic toxicity and very low hatching success were observed when they were exposed to photoenhanced bunker oil (Incardona et al., 2012a; Incardona et al., 2012b). In these studies, the herring embryos developed to the hatching stage before suffering extensive tissue deterioration (Incardona et al., 2012b). In contrast, we observed increased mortality in the oil-UV treatments from exposure start to hatching. However, the mortality increased during the late embryonic stage after onset of cardiac function (120 hpes (8 dpf) and onward).

Co-exposure with oil and UV lowers the threshold for adverse effects significantly. The non-linear regression analysis for mortality was performed with the measured water concentration of totPAH and tissue concentration (bodyburden, BB) of totPAH (Dataset S1 and S2) and not nominal crude oil concentrations. The treatment with crude oil and UV resulted in a 2.5–3 times lower 50 % lethal concentration (LC50) (Fig. 6, Table S3). Similarly, the BMD50 values of 650 ng totPAH/L and 521 μg totPAH/kg ww in the no UV treatment dropped to 261 ng totPAH/L and 162 μg totPAH/kg ww in the UV treatment. Calculations of LC50, BMD10 and BMD50 with lower and upper confidence limits are given in Fig. S5, Fig. S6, and Table S4. Although single PAHs such as the three ring PAH anthracene can exhibit a UV-enhanced toxicity of 1000 fold, others such as phenanthrene do not exhibit toxicity. In mixtures like crude oil, the phototoxicity is additive and can be predicted based on physiochemical characteristics (Barron, 2017; Finch et al., 2017). Various petroleum products may, therefore, exhibit zero to an increase in phototoxicity based on the content of photoexcitable PAHs (Barron, 2017). Here we show that even though the fraction of photoexcitable PAHs in crude oil is very small (<1 %), it is still sufficient to significantly increase the toxicity by 3-fold. These reported values are for acute mortality; note that sublethal toxic effects in later larval stages (30 dph) of Atlantic haddock, such as reduced swimming performance, were seen after exposure to levels as low as 0.1 μg PAH/L (Cresci et al., 2020).

Spinal and eye deformities were seen in all UV treatments including C-UV (Fig. 7). UV radiation alone increases the occurrence of several embryonic malformations, such as spinal deformities, minor spinal bending and enlarged pericardial sacs (Alves and Agustí, 2020). Increasing incidence of spinal and craniofacial abnormalities coincided with increasing oil concentration. In the H-oil-noUV all the investigated larvae had spinal abnormalities and 87 % had the most severe phenotype (hunchback). Similarly, the most severe eye deformities (protruding lens) were more common with increasing oil concentration (Fig. 7). Medium and high concentrations (noUV) showed reduced length, body/yolk area, eye area, ethmoid plate size and jaw length. In the low concentrations spinal and eye deformities were more frequent in the co-exposed treatments. However, variation in morphological endpoints were seen, but not in a clear dose response fashion. The response rather followed the changes of *cyp1a* and *cyp1c* expression in the treatments, highlighting them as valid internal biomarkers for oil toxicity (Table S2, Figs. 2C, 3A, C and S3).

To detect more subtle impacts on cardiac development, the area of the ventricle was measured (Fig. 8). The C-UV had significantly larger ventricles than the C-noUV. This faster heart growth with UV could be explained through vitamin D pathways. Photolytic transformation of 7-dehydrocholesterol (7-DHC) to D-vitamin in skin and tissues is induced by UV radiation (Wacker and Holick, 2013). UV-exposure in laboratory studies show that both early life stages and adult fish have the capability

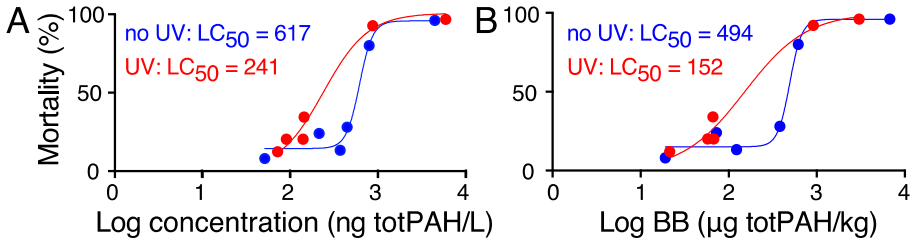

Fig. 6. Mortality in Atlantic haddock at hatch (0 dph) and calculation of LC50 in treatments without (blue) and with (red) UV. A) Non-linear regression of mortality vs water concentration (µg totPAH/L). B) Non-linear regression of mortality vs body burden (BB) (µg totPAH/kg ww).

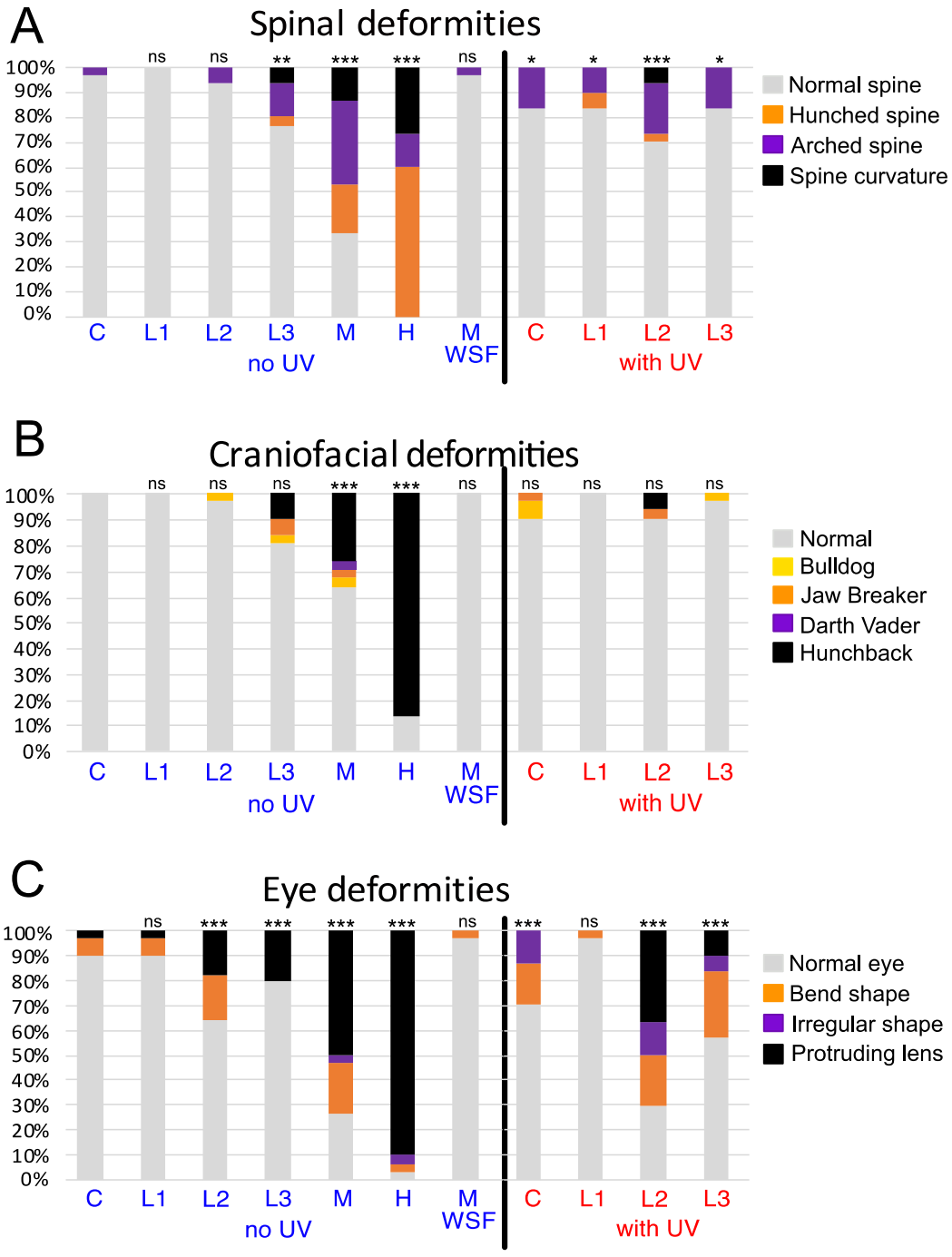

Fig. 7. Spinal, craniofacial and eye deformities in 3 dph Atlantic haddock in the oil exposure treatments with and without UV. A) Spinal deformities, B) craniofacial deformities, C) eye deformities. Statistical difference from C-no-UV was tested with Chi-square, and ** indicates $p < 0.01$. Number of animals = 30 for spinal and craniofacial and 28–30 for eye deformities (L3-oil-noUV = 28 and UV-C = 29). No larvae from M-oil UV and H-oil-UV survived to 3 dph.

to perform photolytic transformation of 7DHC (Lock et al., 2010). Many tissues respond to vitamin D treatment. In zebrafish, vitamin D activates cardiomyocyte proliferation and regulates cardiac size (Han et al., 2019). Thus, the increased ventricle size of the C-UV animals may be induced by increased photolytic production of vitamin D.

Ventricle area was also affected in both the oil and oil-UV treatments. For example, in the oil treatments, the area of the ventricle was reduced in M-oil-noUV and H-oil-noUV (Fig. 8). In the oil-UV treatments, all had reduced ventricle size compared to C-UV, but only L3-oil-UV treatment exhibited ventricle areas smaller than C-noUV (Fig. 8). Previous findings indicate that exposure to crude oil induces cardiac abnormalities in fish (Sørhus et al., 2021a; Sørhus et al., 2016; Sørhus et al., 2021b), creating altered shape, reduced thickness of compact myocardium and hypertrophic changes in the spongy, trabeculated myocardium (Gardner et al., 2019; Hicken et al., 2011; Incardona et al., 2015). The reduced ventricle sizes we observed follow these findings. Several mechanisms underly the crude oil induced cardiac functional and morphological defects (Brette et al., 2014; Gardner et al., 2019; Sørhus et al., 2017; Wincent et al., 2015; Xiong et al., 2008), including oxidative stress (Takimoto and Kass, 2007). UV co-exposure with crude oil induced oxidative stress pathways in cod (Aranguren-Abadía et al., 2021). In mahi-mahi (*Coryphaena hippurus*), UV radiation exacerbated oil induced cardiotoxicity (Sweet et al., 2017). In the present work, the negative effects of crude oil toxicity and oxidative stress overshadow the potentially positive effect of UV on heart growth. Altered cardiac shape and size may have detrimental consequences later in life, reducing swimming capacity (Hicken et al., 2011; Incardona et al., 2015), and possibly also predator avoidance and feeding behavior.

3.5. The importance of including phototoxicity in risk assessments

Assessing the risk of opening spawning areas for oil exploration should include as many of the relevant factors as possible. Species with translucent pelagic life stages are at the highest risk to be subjected to both UV and oil spills (Barron et al., 2008). Phototoxicity is, therefore, one such factor and empirical data from experiments such as those reported here are crucial input to risk assessment models. UV-radiation on the spawning grounds in Arctic areas is high during the spawning period (March–April) of Atlantic haddock. For example, in the Lofoten islands region the beginning of March has approx. 10 h of daylight, while late April has 18 h of daylight. Thus, incorporating knowledge about UV induced phototoxicity in risk assessment models is extremely relevant in this region. Several species spawning in this area, including haddock and cod, have pelagic eggs and larvae (Olsen et al., 2010). Haddock and cod eggs are spawned at depths of between 50 and 200 m and rise to the surface during the embryonic stage (Solemdal et al., 1997). The eggs and larvae are, therefore, exposed to UV radiation during at least part of their embryonic and larval stages (Kuhn et al., 2000).

4. Conclusions

In this study we showed that exposing haddock embryos to crude oil in combination with UV radiation resulted in severe tissue necrosis and edema formation. This suggests that phototoxicity has high relevance for acute embryotoxicity in the oil-UV exposure reducing LC50 to 0.24 μg totPAH/L. In addition, we observed sublethal morphological changes in the heart following low grade exposures (0.09–0.14 μg totPAH/L) in combination with UV. Minor changes in heart shape and size affect swimming performance during the juvenile stages (Hicken et al., 2011; Incardona et al., 2012a) and may have detrimental consequences for juvenile survival in the wild. Decreased individual survival over time could have a negative impact on stock population.

1 **Supplementary materials and methods.**
Details regarding RNA extraction and RT-qPCR.
2 **Supplementary figures.**
Descriptive images of phenotypes.
Timeline, uptake of PAHs.
Gene expression changes in all treatments at 72 hpes.
Acute embryonic mortality.
Models for calculation of BMD10 and BMD50.
3 **Supplementary tables.**
Primers for RT-qPCR.
Morphometrics at 3 dph.
Nonlinear fit mortality vs log concentration and log bodyburden.
Accepted models for calculation of BMD10 and BMD50.
4 **Supplementary datasets.**
Lists of content of PAHs in water and tissue at 72 hpes (all treatments) and all timepoints (C- and M-treatments).
5 **Supplementary video.**
Six concatenated cardiac videos for C, M and H treatments at 120 hpes.

Supplementary data to this article can be found online at https://doi.org/10.1016/j.scitotenv.2022.160080.

CRediT authorship contribution statement

All authors have given approval to the final version of the manuscript. **Elin Sørhus.**: Designed the study; collected, analyzed, and interpreted the data; and wrote the paper. **Carey E. Donald.**: Collection, analysis and

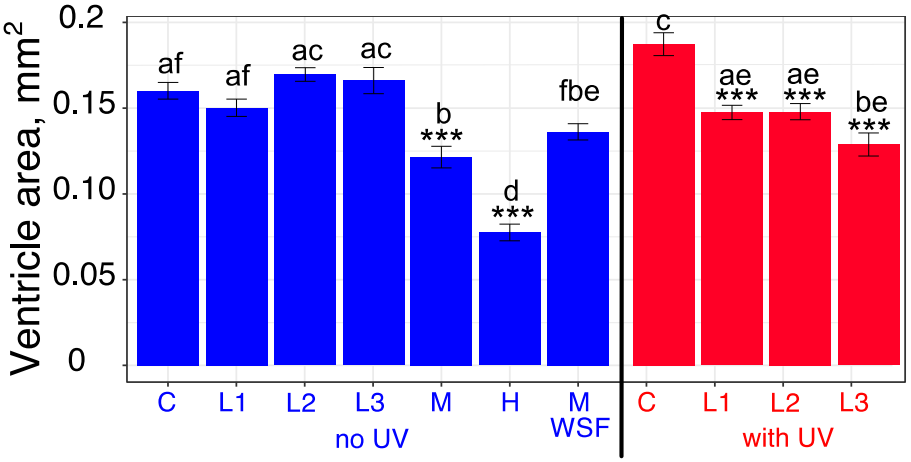

Fig. 8. Area of ventricle in 3 days post hatch Atlantic haddock larvae. Statistical differences between treatments and control (noUV-C or UV-C) were tested with one-way ANOVA with Dunnett's multiple comparison, and significant differences are indicated by $^{**}p < 0.01$ and $^{***}p < 0.001$. Differences between all treatments were tested for using Tukey-Kramer's multiple comparison. Differences are indicated by different letters. No larvae from M-oil-UV and H-oil-UV survived to 3 dph.

interpretation of data, review & editing. **Charlotte L. Nakken**: Collection, analysis and interpretation of data. **Prescilla Perrichon**: Collection of data, review & editing. **Caroline M.F. Durif**: Methodology, collection of data, review & editing. **Steven Shema**: Methodology, collection of data. **Howard I. Browman**: Conceptualization, methodology, review & editing. **Anne Berit Skiftesvik**: Methodology. **Kai K. Lie**: Interpretation of data, review & editing. **Josef D. Rasinger**: Analysis and interpretation of data. **Mette H.B. Müller**: Collection and interpretation of data, writing of methodology. **Sonnich Meier**: Conceptualization, methodology, collection of data, funding acquisition, review and editing.

Data availability

Data will be made available on request.

Declaration of competing interest

The authors declare that they have no known competing financial interests or personal relationships that could have appeared to influence the work reported in this paper.

Acknowledgments

We thank Margareth Møgster and Stig Ove Utskot, the technical staff of the Institute of Marine Research, Austevoll Aquaculture Research Station for their assistance with breeding and management of the fish. Thanks also to Lene Hermansen and Hilde Kolstad at Imaging Centre, NMBU, for SEM support. This work was financed by the Research Council of Norway (Project no. 267820, EGGTOX, www.forskningsradet.no) and the Institute of Marine Research, Norway. The funders had no role in study design, data collection and analysis, decision to publish, or preparation of the manuscript.

References

Adams, J., Bornstein, J.M., Munno, K., Hollebone, B., King, T., Brown, R.S., Hodson, P.V., 2014. Identification of compounds in heavy fuel oil that are chronically toxic to rainbow trout embryos by effects-driven chemical fractionation. Environ. Toxicol. Chem. 33, 825–835.

Allan, S.E., Smith, B.W., Anderson, K.A., 2012. Impact of the Deepwater Horizon oil spill on bioavailable polycyclic aromatic hydrocarbons in Gulf of Mexico coastal waters. Environ. Sci. Technol. 46, 2033–2039.

Alves, R.N., Agustí, S., 2020. Effect of ultraviolet radiation (UVR) on the life stages of fish. Rev. Fish Biol. Fish. 30, 335–372.

Aranguren-Abadía, L., Yadetie, F., Donald, C.E., Sørhus, E., Myklatun, L.E., Zhang, X., Lie, K.K., Perrichon, P., Nakken, C.L., Durif, C., Shema, S., Browman, H.I., Skiftesvik, A.B., Goksøyr, A., Meier, S., Karlsen, O.A., 2021. Photo-enhanced toxicity of crude oil on early developmental stages of Atlantic cod (Gadus morhua). Sci. Total Environ. 807, 150697.

Bagur, R., Hajnóczky, G., 2017. Intracellular Ca(2+) sensing: its role in calcium homeostasis and signaling. Mol. Cell 66, 780–788.

Barron, M.G., 2017. Photoenhanced toxicity of petroleum to aquatic invertebrates and fish. Arch. Environ. Contam. Toxicol. 73, 40–46.

Barron, M.G., Carls, M.G., Short, J.W., Rice, S.D., 2003. Photoenhanced toxicity of aqueous phase and chemically dispersed weathered Alaska North Slope crude oil to Pacific herring eggs and larvae. Environ. Toxicol. Chem. 22, 650–660.

Barron, M.G., Carls, M.G., Short, J.W., Rice, S.D., Heintz, R.A., Rau, M., Di Giulio, R., 2005. Assessment of the phototoxicity of weathered Alaska North Slope crude oil to juvenile pink salmon. Chemosphere 60, 105–110.

Barron, M.G., Vivian, D., Yee, S.H., Diamond, S.A., 2008. Temporal and spatial variation in solar radiation and photoenhanced toxicity risks of spilled oil in Prince William Sound, Alaska,USA. Environ. Toxicol. Chem. 27, 727–736.

Bertilsson, S., Widenfalk, A., 2002. Photochemical degradation of PAHs in freshwaters and their impact on bacterial growth – influence of water chemistry. Hydrobiologia 469, 23–32.

Boehm, P.D., Murray, K.J., Cook, L.L., 2016. Distribution and attenuation of polycyclic aromatic hydrocarbons in Gulf of Mexico seawater from the Deepwater Horizon oil accident. Environ. Sci. Technol. 50, 584–592.

Brette, F., Machado, B., Cros, C., Incardona, J.P., Scholz, N.L., Block, B.A., 2014. Crude oil impairs cardiac excitation-contraction coupling in fish. Science 343, 772–776.

Brown, J.H., 2014. Why are there so many species in the tropics? J. Biol. Chem. 41, 8–22.

Carls, M.G., Meador, J.P., 2009. A perspective on the toxicity of petrogenic PAHs to developing fish embryos related to environmental chemistry. Hum. Ecol. Risk. Assess. 15, 1084–1098.

Chilakamarthi, U., Giribabu, L., 2017. Photodynamic therapy: past, present and future. Chem. Rev. 17, 775–802.

Cresci, A., Browman, H.I., Skiftesvik, A.B., Shema, S., Bjelland, R., Durif, C., Foretich, M., Di Persia, C., Lucchese, V., Vikebø, F., Sorhus, E., 2020. Effects of exposure to low concentrations of oil on expression of cytochrome P4501a and routine swimming speed of Atlantic haddock (Melanogrammus aeglefinus) larvae in situ. Environ. Sci. Technol. 54, 13879–13887.

Date, T.a., 2021. Lofoten, Nordland Fylke, Norge- Soloppgang, solnedgang og dagens lengde.

Edinger, A.L., Thompson, C.B., 2004. Death by design: apoptosis, necrosis and autophagy. Curr. Opin. Cell Biol. 16, 663–669.

Edmunds, R.C., McIntyre, J.K., Luckenbach, J.A., Baldwin, D.H., Incardona, J.P., 2014. Toward enhanced MIQE compliance: reference residual normalization of qPCR gene expression data. J. Biomol. Tech. 25, 54–60.

Ermak, G., Davies, K.J., 2002. Calcium and oxidative stress: from cell signaling to cell death. Mol. Immunol. 38, 713–721.

Finch, B.E., Marzooghi, S., Di Toro, D.M., Stubblefield, W.A., 2017. Evaluation of the phototoxicity of unsubstituted and alkylated polycyclic aromatic hydrocarbons to mysid shrimp (Americamysis bahia): validation of predictive models. Environ. Toxicol. Chem. 36, 2043–2049.

Fridgeirsson, E., 1978. Embryonic development of five species of gadoid fishes in Icelandic waters. Rit Fiskeideildar 5, 1–68.

Gardner, L.D., Peck, K.A., Goetz, G.W., Linbo, T.L., Cameron, J.R., Scholz, N.L., Block, B.A., Incardona, J.P., 2019. Cardiac remodeling in response to embryonic crude oil exposure involves unconventional NKX family members and innate immunity genes. J. Exp. Biol. 222.

Goksøyr, A., 1995. Use of cytochrome P450 1A (CYP1A) in fish as a biomarker of aquatic pollution. Arch. Toxicol. Supplement. 17, 80–95.

Görlach, A., Bertram, K., Hudecova, S., Krizanova, O., 2015. Calcium and ROS: a mutual interplay. Redox Biol. 6, 260–271.

Guo, C., Sun, L., Chen, X., Zhang, D., 2013. Oxidative stress, mitochondrial damage and neurodegenerative diseases. Neural Regen. Res. 8, 2003–2014.

Hall, T.E., Smith, P., Johnston, I.A., 2004. Stages of embryonic development in the Atlantic cod Gadus morhua. J. Morphol. 259, 255–270.

Han, Y., Chen, A., Umansky, K.B., Oonk, K.A., Choi, W.Y., Dickson, A.L., Ou, J., Cigliola, V., Yifa, O., Cao, J., Tornini, V.A., Cox, B.D., Tzahor, E., Poss, K.D., 2019. Vitamin D stimulates cardiomyocyte proliferation and controls organ size and regeneration in zebrafish. Dev. Cell 48, 853–863.e855.

Hansen, B.H., Sørensen, L., Carvalho, P.A., Meier, S., Booth, A.M., Altin, D., Farkas, J., Nordtug, T., 2018. Adhesion of mechanically and chemically dispersed crude oil droplets to eggs of Atlantic cod (Gadus morhua) and haddock (Melanogrammus aeglefinus). Sci. Total Environ. 640–641, 138–143.

Hansen, B.H., Parkerton, T., Nordtug, T., Storseth, T.R., Redman, A., 2019. Modeling the toxicity of dissolved crude oil exposures to characterize the sensitivity of cod (Gadus morhua) larvae and role of individual and unresolved hydrocarbons. Mar. Pollut. Bull. 138, 286–294.

Harding, L.B., Tagal, M., Ylitalo, G.M., Incardona, J.P., Davis, J.W., Scholz, N.L., McIntyre, J.K., 2020. Urban stormwater and crude oil injury pathways converge on the developing heart of a shore-spawning marine forage fish. Aquat. Toxicol. 229, 105654.

Harmati, M., Gyukity-Sebestyen, E., Dobra, G., Janovak, L., Dekany, I., Saydam, O., Hunyadi-Gulyas, E., Nagy, I., Farkas, A., Pankotai, T., Ujfaludi, Z., Horvath, P., Piccinini, F., Kovacs, M., Biro, T., Buzas, K., 2019. Small extracellular vesicles convey the stress-induced adaptive responses of melanoma cells. Sci. Rep. 9, 15329.

Hicken, C.E., Linbo, T.L., Baldwin, D.H., Willis, M.L., Myers, M.S., Holland, L., Larsen, M., Stekoll, M.S., Rice, S.D., Collier, T.K., Scholz, N.L., Incardona, J.P., 2011. Sublethal exposure to crude oil during embryonic development alters cardiac morphology and reduces aerobic capacity in adult fish. Proc. Nat. Acad. Sci. U. S. A. 108, 7086–7090.

Incardona, J.P., Vines, C.A., Anulacion, B.F., Baldwin, D.H., Day, H.L., French, B.L., Labenia, J.S., Linbo, T.L., Myers, M.S., Olson, O.P., Sloan, C.A., Sol, S., Griffin, F.J., Menard, K., Morgan, S.G., West, J.E., Collier, T.K., Ylitalo, G.M., Cherr, G.N., Scholz, N.L., 2012a. Unexpectedly high mortality in Pacific herring embryos exposed to the 2007 Cosco Busan oil spill in San Francisco Bay. Proc. Nat. Acad. Sci. U. S. A. 109, E51–E58.

Incardona, J.P., Vines, C.A., Linbo, T.L., Myers, M.S., Sloan, C.A., Anulacion, B.F., Boyd, D., Collier, T.K., Morgan, S., Cherr, G.N., Scholz, N.L., 2012b. Potent phototoxicity of marine bunker oil to translucent herring embryos after prolonged weathering. Plos one 7.

Incardona, J.P., Carls, M.G., Holland, L., Linbo, T.L., Baldwin, D.H., Myers, M.S., Peck, K.A., Tagal, M., Rice, S.D., Scholz, N.L., 2015. Very low embryonic crude oil exposures cause lasting cardiac defects in salmon and herring. Sci. Rep. 5, 13499.

Incardona, J.P., Linbo, T.L., French, B.L., Cameron, J., Peck, K.A., Laetz, C.A., Hicks, M.B., Hutchinson, G., Allan, S.E., Boyd, D.T., Ylitalo, G.M., Scholz, N.L., 2021. Low-level embryonic crude oil exposure disrupts ventricular ballooning and subsequent trabeculation in Pacific herring. Aquat. Toxicol. 235, 105810.

Ji, K., Seo, J., Liu, X., Lee, J., Lee, S., Lee, W., Park, J., Khim, J.S., Hong, S., Choi, Y., Shim, W.J., Takeda, S., Giesy, J.P., Choi, K., 2011. Genotoxicity and endocrine-disruption potentials of sediment near an oil spill site: two years after the Hebei Spirit oil spill. Environ. Sci. Technol. 45, 7481–7488.

Kuhn, P.S., Browman, H.I., Davis, R.F., Cullen, J.J., McArthur, B.L., 2000. Modeling the effects of ultraviolet radiation on embryos of Calanus finmarchicus and Atlantic cod (Gadus morhua) in a mixing environment. Limnol. Oceanogr. 45, 1797–1806.

Kvæstad, B., Hansen, B.H., Davies, E., 2022. Automated morphometrics on microscopy images of Atlantic cod larvae using Mask R-CNN and classical machine vision techniques. MethodsX 9, 101598.

Laurel, B.J., Copeman, L.A., Iseri, P., Spencer, M.L., Hutchinson, G., Nordtug, T., Donald, C.E., Meier, S., Allan, S.E., Boyd, D.T., Ylitalo, G.M., Cameron, J.R., French, B.L., Linbo, T.L., Scholz, N.L., Incardona, J.P., 2019. Embryonic crude oil exposure impairs growth and lipid allocation in a keystone arctic forage fish. iScience 19, 1101–1113.

Leads, R.R., Magnuson, J.T., Lucero, J., Lund, A.K., Schlenk, D., Chavez, J.R., Roberts, A.P., 2022. Transcriptomic responses and apoptosis in larval red drum (Sciaenops ocellatus) co-exposed to crude oil and ultraviolet (UV) radiation. Mar. Pollut. Bull. 179, 113684.

Li, T., Zhao, X.P., Wang, L.Y., Gao, S., Zhao, J., Fan, Y.C., Wang, K., 2013. Glutathione S-transferase P1 correlated with oxidative stress in hepatocellular carcinoma. Int. J. Med. Sci. 10, 683–690.

Lock, E.J., Waagbø, R., Wendelaar Bonga, S., Flik, G., 2010. The significance of vitamin D for fish: a review. Aquac. Nutr. 16, 100–116.

Magi, E., Di Carro, M., 2018. Marine environment pollution: the contribution of mass spectrometry to the study of seawater. Mass Spectrom. Rev. 37, 492–512.

Manney, G.L., Santee, M.L., Rex, M., Livesey, N.J., Pitts, M.C., Veefkind, P., Nash, E.R., Wohltmann, I., Lehmann, R., Froidevaux, L., Poole, L.R., Schoeberl, M.R., Haffner, D.P., Davies, J., Dorokhov, V., Gernandt, H., Johnson, B., Kivi, R., Kyrö, E., Larsen, N., Levelt, P.F., Makshtas, A., McElroy, C.T., Nakajima, H., Parrondo, M.C., Tarasick, D.W., von der Gathen, P., Walker, K.A., Zinoviev, N.S., 2011. Unprecedented Arctic ozone loss in 2011. Nature 478, 469–475.

Meador, J.P., Nahrgang, J., 2019. Characterizing crude oil toxicity to early-life stage fish based on a complex mixture: are we making unsupported assumptions? Environ. Sci. Technol. 53, 11080–11092.

Misund, O.A., Olsen, E., 2013. Lofoten-Vesterålen: for cod and cod fisheries, but not for oil? ICESJ. Mar. Sci. 70, 722–725.

Morrison, C., Bird, C., O'Neil, D., Leggiadro, C., Martin-Robichaud, D., Rommens, M., Waiwood, K., 1999. Structure of the egg envelope of the haddock, Melanogrammus aeglefinus, and effects of microbial colonization during incubation. Can. J. Zool. 77, 890–901.

Nordtug, T., Olsen, A.J., Altin, D., Meier, S., Overrein, I., Hansen, B.H., Johansen, O., 2011. Method for generating parameterized ecotoxicity data of dispersed oil for use in environmental modelling. Mar. Pollut. Bull. 62, 2106–2113.

Olsen, E., Aanes, S., Mehl, S., Holst, J.C., Aglen, A., Gjosaeter, H., 2010. Cod, haddock, saithe, herring, and capelin in the Barents Sea and adjacent waters: a review of the biological value of the area. ICES J. Mar. Sci. 67, 87–101.

Oppen-Berntsen, D.O., Helvik, J.V., Walther, B.T., 1990. The major structural proteins of cod (Gadus morhua) eggshells and protein crosslinking during teleost egg hardening. Dev. Biol. 137, 258–265.

Ott, M., Gogvadze, V., Orrenius, S., Zhivotovsky, B., 2007. Mitochondria, oxidative stress and cell death. Apoptosis 12, 913–922.

Pasparakis, C., Esbaugh, A.J., Burggren, W., Grosell, M., 2019. Impacts of Deepwater Horizon oil on fish. Comp. Biochem. Physiol. C: Toxicol. Pharmacol. 224, 108558.

Perrichon, P., Mager, E.M., Pasparakis, C., Stieglitz, J.D., Benetti, D.D., Grosell, M., Burggren, W.W., 2018. Combined effects of elevated temperature and Deepwater Horizon oil exposure on the cardiac performance of larval mahi-mahi, Coryphaena hippurus. Plos one 13.

Peterson, C.H., Rice, S.D., Short, J.W., Esler, D., Bodkin, J.L., Ballachey, B.E., Irons, D.B., 2003. Long-term ecosystem response to the Exxon Valdez oil spill. Science 302, 2082–2086.

Roberts, A.P., Alloy, M.M., Oris, J.T., 2017. Review of the photo-induced toxicity of environmental contaminants. Comp. Biochem. Physiol. C: Toxicol. Pharmacol. 191, 160–167.

Schneider, C.A., Rasband, W.S., Eliceiri, K.W., 2012. NIH image to ImageJ: 25 years of image analysis. Nat. Methods 9, 671–675.

Solemdal, P., Mukhina, N., Knutsen, T., Bjørke, H., Fossum, P., 1997. Maturation, spawning and egg drift of Arcto-Norwegian haddock (Melanogrammus aeglefinus). Icthyoplankton Ecology. University college Galway, Ireland.

Solsvik, T., 2022. Norway plans to expand Arctic oil and gas drilling in new licensing round, Reuters. Reuters. https://www.reuters.com/business/energy/norway-plans-expand-arctic-oil-gas-drilling-new-licensing-round-2022-03-17/.

Sørensen, L., Meier, S., Mjøs, S.A., 2016. Application of gas chromatography/tandem mass spectrometry to determine a wide range of petrogenic alkylated polycyclic aromatic hydrocarbons in biotic samples. Rapid Commun. Mass Spectrom. 30, 2052–2058.

Sørensen, L., Sørhus, E., Nordtug, T., Incardona, J.P., Linbo, T.L., Giovanetti, L., Karlsen, O., Meier, S., 2017. Oil droplet fouling and differential toxicokinetics of polycyclic aromatic hydrocarbons in embryos of Atlantic haddock and cod. Plosone 12, e0180048.

Sørhus, E., Edvardsen, R.B., Karlsen, O., Nordtug, T., van der Meeren, T., Thorsen, A., Harman, C., Jentoft, S., Meier, S., 2015. Unexpected interaction with dispersed crude oil droplets drives severe toxicity in Atlantic haddock embryos. Plosone 10, e0124376.

Sørhus, E., Incardona, J.P., Karlsen, O., Linbo, T., Sørensen, L., Nordtug, T., van der Meeren, T., Thorsen, A., Thorbjørnsen, M., Jentoft, S., Edvardsen, R.B., Meier, S., 2016. Crude oil exposures reveal roles for intracellular calcium cycling in haddock craniofacial and cardiac development. Sci. Rep. 6, 31058.

Sørhus, E., Incardona, J.P., Furmanek, T., Goetz, G.W., Scholz, N.L., Meier, S., Edvardsen, R.B., Jentoft, S., 2017. Novel adverse outcome pathways revealed by chemical genetics in a developing marine fish. elife 6.

Sørhus, E., Donald, C.E., da Silva, D., Thorsen, A., Karlsen, Ø., Meier, S., 2021a. Untangling mechanisms of crude oil toxicity: linking gene expression, morphology and PAHs at two developmental stages in a cold-water fish. Sci. Total Environ. 757, 143896.

Sørhus, E., Meier, S., Donald, C.E., Furmanek, T., Edvardsen, R.B., Lie, K.K., 2021b. Cardiac dysfunction affects eye development and vision by reducing supply of lipids in fish. Sci. Total Environ. 800, 149460.

Sweet, L.E., Magnuson, J., Garner, T.R., Alloy, M.M., Stieglitz, J.D., Benetti, D., Grosell, M., Roberts, A.P., 2017. Exposure to ultraviolet radiation late in development increases the toxicity of oil to mahi-mahi (Coryphaena hippurus) embryos. Environ. Toxicol.Chem. 36, 1592–1598.

Takimoto, E., Kass, D.A., 2007. Role of oxidative stress in cardiac hypertrophy and remodeling. Hypertension 49, 241–248.

Wacker, M., Holick, M.F., 2013. Sunlight and vitamin D: a global perspective for health. Dermatoendocrinology 5, 51–108.

Wincent, E., Jonsson, M.E., Bottai, M., Lundstedt, S., Dreij, K., 2015. Aryl hydrocarbon receptor activation and developmental toxicity in zebrafish in response to soil extracts containing unsubstituted and oxygenated PAHs. Environ. Sci. Technol. 49, 3869–3877.

Wu, L., Sun, R., Li, Y.X., Sun, C.J., 2019. Sample preparation and analytical methods for polycyclic aromatic hydrocarbons in sediment. Trends Environ. Anal. 24.

Xiong, K.M., Peterson, R.E., Heideman, W., 2008. Aryl hydrocarbon receptor-mediated down-regulation of Sox9b causes jaw malformation in zebrafish embryos. Mol. Pharmacol. 74, 1544–1553.